Extraordinary boulder transport by storm waves (West of Ireland, Winter 2013–2014), and criteria for analysing coastal boulder deposits

Article *in* Earth-Science Reviews · December 2017

DOI: 10.1016/j.earscirev.2017.12.014

Earth-Science Reviews 177 (2018) 623–636

Contents lists available at ScienceDirect

Earth-Science Reviews

journal homepage: www.elsevier.com/locate/earscirev

Extraordinary boulder transport by storm waves (west of Ireland, winter 2013–2014), and criteria for analysing coastal boulder deposits

Rónadh Cox*, Kalle L. Jahn, Oona G. Watkins, Peter Cox

Geosciences Department, Williams College, Williamstown, MA 01267, United States

ARTICLE INFO

Keywords:
Coastal boulder deposits
Storm waves
Coastal erosion
Megagravel
Coastal hazard
Coastal geomorphology

ABSTRACT

Before-and-after photos of supratidal coastal boulder deposits (CBD) in the west of Ireland show that storms in the winter of 2013–2014 transported boulders at elevations up to 29 m above high water, and at inland distances up to 222 m. Among the clasts transported are eighteen weighing more than 50 t, six of which exceed 100 t. The largest boulder moved during those storms weighs a fairly astonishing 620 t.

The boulders moved in these recent storms provide pinning points for mapping storm-wave energies on coasts: their topographic positions mark elevations and distances inland reached by wave energies sufficient to dislocate those specific masses. Taken together, the CBD data reveal general relationships that shed light on storm-wave hydrodynamics. These include a robust correlation (inverse exponential) between maximum boulder mass transported and emplacement height above high water: the greater the elevation, the smaller the maximum boulder size, with a dependency exponent of about -0.2 times the elevation (in metres). There is a similar relationship, although with a much smaller rate-of-change (exponent -0.02), between boulder mass and distance inland, which holds from the shoreline in to about 120 m. Coastal steepness (calculated as the ratio of elevation to inland distance) seems to exert the strongest control, with an inverse power-law relationship between maximum boulder mass and slope ratio: the more gentle the topography, the larger the moved boulders.

Quantifying CBD dynamics helps us understand the transmission of wave energies inshore during high-energy storm events. The transported boulders documented here are larger than many of those interpreted to have been moved by tsunami in other locations, which means that boulder size alone cannot be used as a criterion for distinguishing between tsunami and storm emplacement of CBD. The biggest blocks—up to 620 t—are new maxima for boulder mass transported by storm waves. We predict, however, that this record will not last long: the 2013–2014 storms were strong but not extreme, and there are larger boulders in these deposits that didn't move on this occasion. Bigger storms will surely move larger clasts, and clasts at greater distances from the shoreline. These measurements and relationships emphasise the extreme power of storm waves impacting exposed coastlines, and require us to rethink the upper limits of storm wave energy at coasts.

1. Introduction

A series of unusually strong storms battered the eastern Atlantic in the winter of 2013–2014. Spectacular photographs of wave impacts on coasts and infrastructure appeared at the time in newspapers and scientific blogs (e.g. Duell and Brady, 2014; Petley, 2014), and resultant geomorphologic effects have been documented in the literature (Castelle et al., 2015; Earlie et al., 2015; Autret et al., 2016; Burvingt et al., 2016; Masselink et al., 2016). But some of the most dramatic changes were not shown in the newspapers. They occurred far from the public eye, on inhospitable and uninhabited rocky coastlines characterised by cliffs and open-ocean deep-water exposure. These are the sites of coastal boulder deposits (CBD: Fig. 1), which are poorly understood piles of clasts (including, in some locations, blocks weighing 10 s to 100 s of tonnes) that can occur at elevations up to 50 m AHW in some places, and can be up to a quarter of a kilometre inland in others (Williams and Hall, 2004).

Large waves can send water surging across coastal platforms or cliff tops, and this flow—referred to as a bore (Hibberd and Peregrine, 1979; Nott, 2003b)—may dislodge and entrain clasts, sweeping them inland. But whether storm waves can generate sufficient force to move very large rocks, or whether the biggest boulders require tsunami to activate them, has been controversial. So although some CBD were interpreted as storm deposits (e.g. Williams and Hall, 2004; Hall et al., 2008; Goto et al., 2010; Hall et al., 2010), the sheer size of many blocks seemed to indicate that storm wave transport was unlikely (Nott, 2003a; Noormets

* Corresponding author.
E-mail address: rcox@williams.edu (R. Cox).

https://doi.org/10.1016/j.earscirev.2017.12.014
Received 30 April 2017; Received in revised form 8 December 2017; Accepted 18 December 2017
Available online 24 December 2017

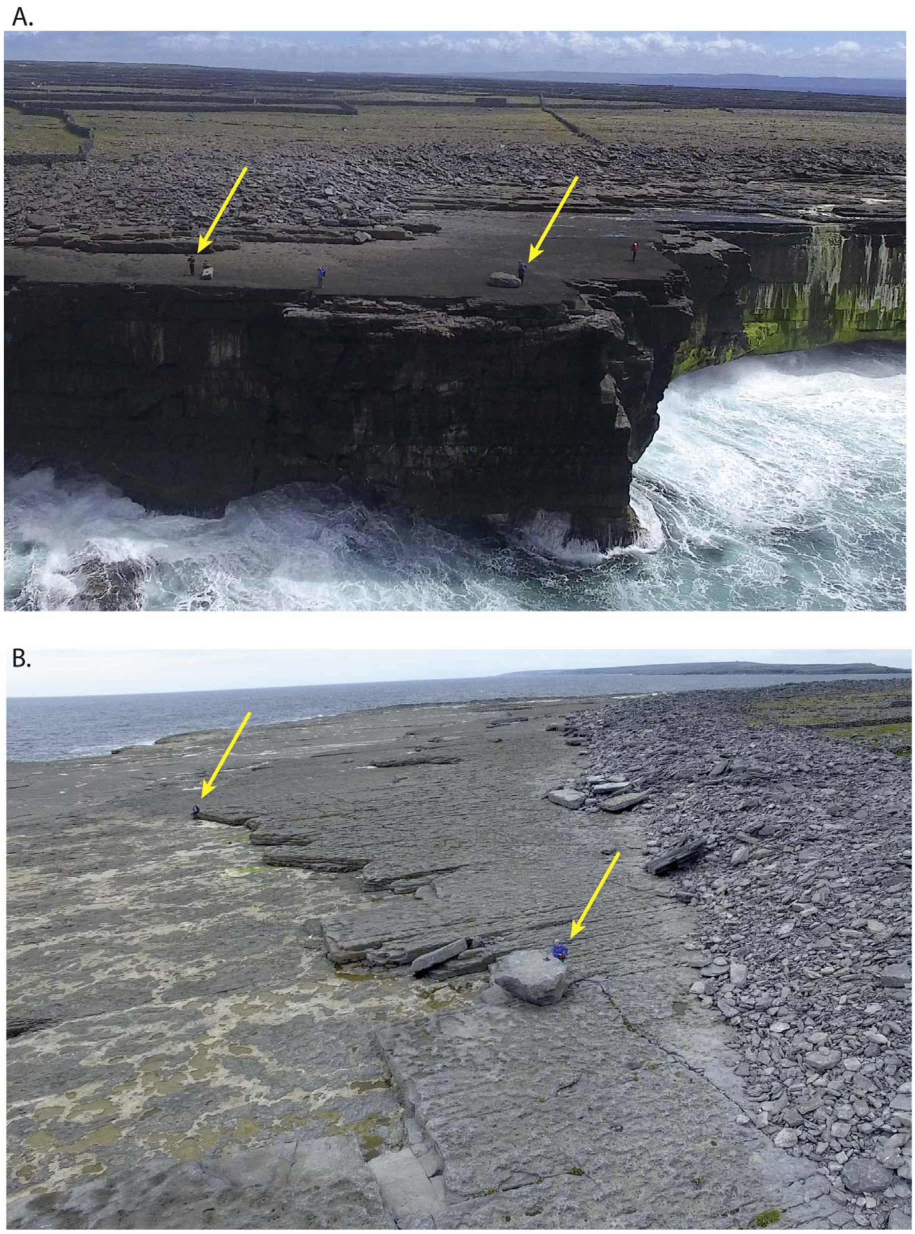

Fig. 1. Coastal boulder deposits (CBD) in different settings. Arrows indicate people (adults) for scale. **A**. Cliff-top CBD at locations 68–69 (Fig. 3, Supplementary Table 1) on Inishmaan. The cliffs in this field of view are above high water, and the seaward edge of the boulder ridge is 32–42 m inland from the cliff edge. **B**. Locations 47–49 on Inishmaan are at the back of a broad, gently sloping coastal platform. The seaward edge of the boulder ridge is 10–11 m AHW and 150–160 m inland, and the ridge itself is about 3 m tall. The paler-coloured bedrock at the toe of the boulder pile was newly exposed when this CBD migrated inland by 1–2 m in winter 2013–2014. The large isolated boulder in the foreground (with person next to it) has mass ≈ 19 t (see Table 1, Boulder 3). Both photographs were taken in summer 2016. In addition to showcasing different kinds of CBD setting, these images speak to ongoing boulder transport: the isolated clasts with people next to them (two in **A**, one in **B**) all moved between 2014 and 2016. The boulder at the right-hand arrow in **A** appeared in Winter 2015, and is one of the mass-estimate test boulders listed in Table 1. Additional site images can be found in Supplemental Figs. 1–4.

et al., 2004; Scheffers et al., 2009; Hoffmann et al., 2013; Scheffers and Kinis, 2014), and so there was no consensus on emplacement mechanism. Only very recently have before-and-after observations proven that storm waves can and do move giant boulders (May et al., 2015; Cox et al., 2016; Kennedy et al., 2017), but still we know very little about the dynamics of block and boulder transport, or about how storm wave energy is distributed with respect to coastal topography.

Archives of high-energy wave events, CBD are not activated very often (Hansom and Hall, 2009; Scheffers et al., 2010). Because of this, and because of their remote locations, few direct observations of clast motions exist. The lack of data has led some workers to argue that large boulders have stayed in place during hundreds or thousands of years of storm-wave attack (Scheffers and Kinis, 2014), and to conclude that "the larger 80% of individual boulders in ridges have not been moved recently or within the last centuries" (Erdmann et al., 2017). The winter of 2013–2014 provided a unique opportunity to examine the response of CBD to high-energy storm waves, because severe storms struck an area for which detailed observations had been built up over the previous decade (e.g. Williams and Hall, 2004; Zentner, 2009; Cox et al., 2012; Jahn, 2014). Rapid-response field work demonstrated that not only were western Ireland's CBD substantially reorganised, but that large new boulders were created and added to the deposits (Cox et al., 2014; Cox et al., 2016). Documenting these changes matters because CBD, in the west of Ireland and elsewhere in the world, are at the centre of ongoing debate about the absolute power of storm waves.

In this contribution we review CBD in general: the different kinds, where they occur, and the background to the storm-versus-tsunami debate. We then report the storm-driven displacement of 1153 individual boulders — including some with masses in the 100s of tonnes—on Ireland's western coasts during the winter of 2013–2014. We relate boulder movements to coastal topography and derive quantitative relationships that may be used as baseline comparison measures for CBD worldwide**.** The before-and-after comparisons not only encompass a spectrum of topographic settings—from the tops of sheer cliffs to low-lying coastal platforms—but incorporate the full range of boulder sizes, permitting detailed quantitative analysis. These data show definitively that storm waves can move blocks > 600 t mass, and that they can transmit forces sufficient to move megagravel at substantial elevations and distances inland.

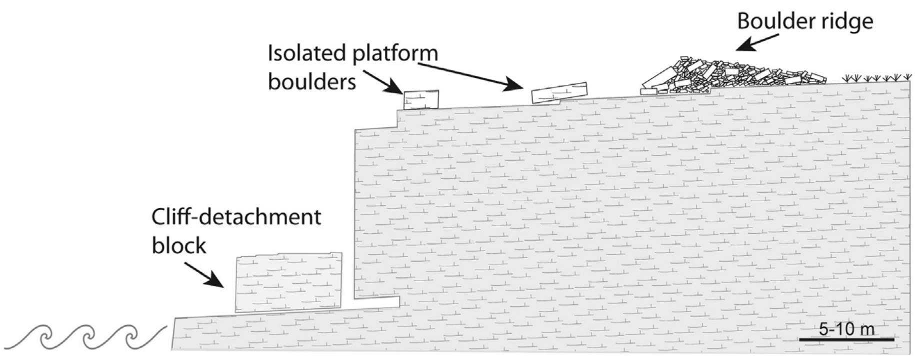

Fig. 2. Diagrammatic representation of the different kinds of CBD. Boulder ridges may form at a range of elevations, from 1 to 50 m AHW and are built of clasts ranging in size from fine pebbles to medium blocks (per the Blair and McPherson, 1999 size scale). Isolated platform boulders are usually large relative to clasts in the ridge (> 95th percentile in grain size). Both boulder ridges and isolated platform boulders are excavated and transported inland by wave, with some component of work done against gravity. Cliff-detachment blocks fall or are separated from superjacent cliff faces, and are moved along the shore platform with little or no vertical component to the transport.

2. Supratidal coastal boulder deposits: an overview

CBD are emplaced by ocean waves above the local high water mark (Fig. 1, and see also Supp. Figs. 1–4). They occur worldwide, mostly along high-energy coastlines exposed to the open ocean (e.g. Nott, 1997; Morton et al., 2008; Etienne and Paris, 2010; Goto et al., 2010; Fichaut and Suanez, 2011; Richmond et al., 2011; May et al., 2015). Some include Very Large Boulders (VLB, defined by Scheffers et al., 2009 as having mass in excess of 50 t), with clasts > 100 t reported from many sites. CBD are found at elevations up to 50 m above high water, and as much as 300 m inland (e.g. Williams and Hall, 2004; Goto et al., 2011; Cox et al., 2012; May et al., 2015; Cox et al., 2017).

CBD include cliff-top deposits (e.g. Hall et al., 2006; Hall et al., 2008) (Fig. 1A), but are not limited to that environment: they also occur in the absence of cliffs, at the back of inclined or stepped coastal platforms (e.g. Scheffers et al., 2010; Hall, 2011; Cox et al., 2012) (Fig. 1B,). Coastal profiles at CBD sites vary (e.g. Suanez et al., 2009; Etienne and Paris, 2010; Cox et al., 2012). Many are steep, with either a single cliff or series of bedrock steps descending to the ocean (Fig. 1A, Supp. Figs. 2, 4); but in other cases the topography can be gradually sloping, with CBD forming a boulder ridge at the back of a broad platform (Fig. 1B. Supp. Figs. 1, 3).

Whatever the local topography, CBD are generally separated from the ocean by a bedrock surface (Hall et al., 2006; Suanez et al., 2009) and are not connected with any kind of beach deposit (Fig. 1). They are distinctly different from those deposits referred to as boulder beaches or storm beaches, which form in the swash zone as higher-energy analogues to sandy beaches (Emery, 1955; Oak, 1984; Lorang, 2000; Buscombe and Masselink, 2006). As they are not graded to the water's edge, and as most are located out of reach of workaday waves, they record extreme wave activity in those locations where they occur.

There are three kinds of supratidal CBD: boulder ridges, isolated platform boulders, and cliff-detachment blocks (Fig. 2). Boulder ridges, which contain most of the CBD material (Fig. 1, Supp. Figs. 1–4), are structured, organised, coast-parallel accumulations (Williams and Hall, 2004; Cox et al., 2012) built of clasts that range from small pebbles to megagravel (sensu Blair and McPherson, 1999). Boulders vary in their degree of rounding, but are angular on average, attesting to infrequent movement (Cox et al., 2017). Size distributions generally show moderate sorting, consistent with organised emplacement by fluid flow (Etienne and Paris, 2010; Cox et al., 2012; Jahn, 2014). Boulder ridges are 1–7 m high and asymmetric, with a more steeply inclined (up to 35°) upstream (ocean side) face and a gentle (< 14°) lee slope that usually grades landward into a scattered boulder field (Hall et al., 2006; Zentner, 2009). They may extend for hundreds of m or even several km along the coast (e.g. on the Aran Islands: Williams and Hall, 2004, Cox et al., 2012), or they may simply form discontinuous clusters (e.g. on Eleuthera in the Bahamas: Kelletat et al., 2004, or on Shetland: Hall et al., 2008). Ridges are separated from the ocean by wave-scoured bedrock, clean of sediment and vegetation, on which large isolated boulders may sit (Hall et al., 2006; Etienne and Paris, 2010).

Isolated platform boulders are usually found seaward of a boulder ridge, sitting on bedrock (Figs. 1, 2, Supp. Fig. 2 and 3). Most are solitary, although small clusters may also occur (Williams and Hall, 2004; Morton et al., 2006). They tend to be bigger than most ridge boulders, and are commonly in the megagravel size category (sensu Blair and McPherson, 1999). The clusters (e.g. Supp. Fig. 3) may in some cases represent former locations of the boulder ridge front, stranded by their greater mass as the rest of the boulder population migrated inland (although this has yet to be demonstrated).

Cliff detachment forms the very largest clasts (masses in the multiple hundreds of tonnes) (Figs. 2, 4, Supp. Fig. 8). These giant blocks calve from the adjacent rock face along planes of weakness that are surely exploited and opened by waves, but with the final separation largely due to gravity. They sit close to sea level. Once separated from the cliff they may simply wear away in place, unless wave energy is sufficient to move them, in which case they may scoot across the platform. In addition to examples described later in this paper, one of the largest clasts transported during Supertyphoon Haiyan (≈ 180 t: May et al., 2015) is an example of a cliff-detachment clast.

Most boulders (cliff-detachment blocks are an exception) are wave-quarried from subjacent supratidal bedrock (Williams and Hall, 2004; Herterich et al., in press). Where deposits sit atop a vertical cliff (Fig. 1 A), clasts come from the upper part of the cliff, extracted and transported inland by the highest-reaching waves. At less-steep sites (e.g. Fig. 1B, Supp. Figs. 1, 3)—where deposits also tend to be farther inland— lithologic comparisons show that most boulders are quarried close to their resting location, by peeling of subjacent bedrock at 10 s to 100 s of m from the ocean (e.g. Supp. Fig. 6, also starred clast in Supp. Fig. 7). Thus boulder creation generally happens quite close to the site of deposition, so although clasts are deposited in many cases quite far inland and well above the high water mark, net transport distances are often not that large.

In exception to that general rule, a small proportion of clasts is sourced at considerable horizontal distance (10s to 100s of m) from the deposition site. These intertidal or subtidal clasts can be recognised by adhering fauna (barnacles, mussels, coralline algae, etc.), or may have other traces of biologic activity, such as borings by sponges or bivalves (Cox et al., 2012; Erdmann et al., 2017). Although attached organisms will decay and fall off with time, the effects of boring organisms persist for much longer. This mechanism for identifying inter- or subtidal clasts is lithology dependent, however: limestones and some sandstones are easily exploited by borers, for example, but volcanic or metamorphic rocks are harder and less soluble; so it may be more difficult to discern whether CBD in those lithologies had submarine sources.

Regardless, however, of whether bedrock is quarried close to the site of deposition or whether excavated blocks are transported long horizontal distances, the wave-generated forces being applied in these supratidal settings are considerable. And (with the exception of cliff-detachment blocks) the work to detach and move these clasts is done against gravity: the vast majority are transported both landward and upward.

2.1. How often do the boulders move?

This is an open question because CBD are activated only by unusually strong waves, they show little or no change from year to year. The biggest boulders can sit unmoved for decades or maybe even centuries (Hansom and Hall, 2009; Scheffers et al., 2010; Hall, 2011; Cox et al., 2012), and as they occur along desolate coastlines where people do not build and spend little time, their transport has generally gone unrecorded. In comparison with other coastal environments, CBD are relatively unstudied, and thus there are few data to illustrate whether, how, and when they move.

2.2. Storms or tsunami?

The oldest CBD observations of which we are aware (Hibbert-Ware, 1822; O'Donovan, 1839; Stevenson, 1845; Kinahan et al., 1878; Süssmilch, 1912) all concluded firmly—based on field observations—that storm waves create and transport boulders weighing many tons. The record include general statements about events such as "the late memorable storm, which hurled the waves in mountains over those high cliffs, (and) cast rocks of amazing size over the lower ones to the east of them" (O'Donovan, 1839), as well as precise determinations, e.g. "In the winter of 1802, a tabular-shaped mass, 8 feet 2 inches by 7 feet, and 5 feet 1 inch thick, was dislodged from its bed, and removed to a distance of from 80-90 feet" (Hibbert-Ware, 1822).

There were few such studies, however, and CBD were largely ignored for most of the 20th century. So when interest arose in late 1990s and early 2000s (with the work of Young et al., 1996; Bryant and Nott, 2001; Scheffers, 2002; Felton and Crook, 2003; Kelletat et al., 2004; Noormets et al., 2004; and Williams and Hall, 2004, among others), there were no long-term observational records on which to draw. Workers trying to interpret CBD therefore had to depend primarily on numerical approaches. A number of innovative studies derived hydrodynamic equations relating boulder masses to the forces required to move them (e.g. Young et al., 1996; Nott, 2003b; Noormets et al., 2004), and used those as the basis for hindcasting wave heights needed. These calculations, when applied to the largest boulders in CBD at various locations, returned storm wave heights that seemed unrealistic in the context of then-available wave spectral data (Nott, 2003a; Noormets et al., 2004), and thus appeared to indicate that storm waves were incapable of emplacing boulders that were very large or too high above sea level. In contrast, the required tsunami heights that fell out of the calculations were far smaller and more credible. Tsunami action was therefore deemed the most likely mechanism for CBD emplacement.

Extensive application of these approaches resulted in interpretation of many CBD as tsunamigenic, or probably tsunamigenic, with hydrodynamic analysis based on boulder size being the most commonly applied determinant (Young et al., 1996; Bryant, 2001; Whelan and Kelletat, 2005; Mastronuzzi et al., 2007; Scicchitano et al., 2007; Barbano et al., 2010; Medina et al., 2011; Mottershead et al., 2014; Prizomwala et al., 2015). Since the CBD themselves showed little evidence for activity on the timescales of investigation, and calculations suggested that storm waves were insufficiently powerful, the conclusion that tsunami were the most likely agents of CBD emplacement seemed reasonable, and persisted in the literature (e.g. Nott, 1997; Bryant and Nott, 2001; Scheffers and Kelletat, 2003; Scheffers et al., 2009).

Other sedimentologic interpretations cascaded from that interpretation, and many characteristics of CBD—including clast size, organisation into sorted groups, imbrication, and supra-tidal location—were asserted to be signatures of tsunami emplacement (Bryant, 2014; Scheffers and Kinis, 2014). In an influential, widely cited paper, Bryant and Nott (2001) concluded that "imbricated boulder piles are the unmistakable signature of tsunami overwash", and Courtney et al. (2012) reported that boulder ridges are frequently taken as diagnostic indicators of tsunami activity. Bryant (2014) asserted that storm waves are unlikely to transport boulders and deposit them in imbricated piles at the top of cliffs, and Scheffers and Kinnis (2014) held that "good imbrication, as well as balancing boulders in delicate positions perched on top of boulder clusters or boulder ridges… are indicative of tsunami impact and exclude storm waves".

Some workers pointed out evidence tying imbricated CBD to storm processes (e.g. Williams and Hall, 2004; Hall et al., 2006; Hansom et al., 2008; Hansom and Hall, 2009; Etienne and Paris, 2010; Hall, 2011). It was also argued that existing hydrodynamic equations largely ignore non-linear effects that can dramatically change wave behaviour, and that they did not adequately capture the complexities of storm-wave dynamics at coasts, which might promote dramatic increases in wave height (e.g. Hansom et al., 2008; Cox et al., 2012). But the tsunami narrative was strong, and in the absence of direct observational data, the numerical arguments were difficult to refute.

The data landscape has changed, however, as our understanding of wave dynamics grows apace. There are more oceanographic data buoys providing more data about wave spectra, and wave modeling codes become ever more sophisticated (e.g. Roland and Ardhuin, 2014; Forget et al., 2015; Beisiegel and Dias, 2017; Brennan et al., 2017). Marine buoy data gathered over the last couple of decades reveal that very large storm waves occur regularly. In the North Atlantic, for example, significant wave heights (SWH)[1] in excess of 18 m have been measured (Turton and Fenna, 2008), with maximum heights up to twice the SWH (Burgers et al., 2008). And it seems that as more data become available, measured wave heights increase in tandem, suggesting that we have not been collecting records for long enough to have gauged near-shore storm wave maxima with any confidence.

The record for highest wave measured offshore of Ireland, for example, keeps going up: from 20.4 m in December 2011 to 23.4 in January 2014, then to 25 m in February 2014 (O'Brien et al., 2013; Met Éireann, 2014; Atan et al., 2016), and most recently to 26.1 m during storm Ophelia in October 2017 (Siggins, 2017). In addition, there is a growing appreciation that interactions at steep coasts can generate very large waves, including "rogue waves", defined as having at least twice the local significant wave height (e.g. Didenkulova and Anderson, 2006; Soomere, 2010; Didenkulova, 2011). The greatest wave amplifications tend to occur at coasts with deep water close to shore (Tsai et al., 2004)—a characteristic of many coastal boulder-ridge sites (Bryant and Nott, 2001; Cox et al., 2012)—and this dovetails with recent modeling work showing that abrupt bathymetric transitions can produce dramatic wave amplifications (e.g. Carbone et al., 2013; Viotti et al., 2014; Viotti and Dias, 2014; Brennan et al., 2017). Finally, the role of infragravity waves, which can magnify these effects by raising the local sea surface several metres, is emerging as important (e.g. Sheremet et al., 2014; Autret et al., 2016).

It is now well demonstrated that storm wave heights—especially when amplified near steep coasts—can be much greater than predicted by simple wave theory (O'Brien et al., 2013; Viotti and Dias, 2014; Akrish et al., 2016). Recent data show unequivocally that storm waves are routinely larger than had previously been recognised (Flanagan et al., 2016; Rueda et al., 2016; Santo et al., 2016). In addition, application of hydrodynamic equations to boulders transported during specific storm events (for which wave heights are known) has shown that hydrodynamic calculations can significantly overestimate the wave heights required to move those blocks (e.g. Switzer and Burston, 2010). Thus cracks have appeared in the argument that storms cannot generate waves sufficiently large to move CBD megaclasts: in fact, they can.

At the same time, direct evidence for storm-wave emplacement of large boulders has accumulated (Courtney et al., 2012). In addition to plastic objects of recent vintage being found inextricably trapped

[1] SWH = 4 × the square root of the variance of the time series of the wave signal, and approximates the mean height of the largest third of waves measured in a given time period. Generally, the height of the largest 1% of waves is ≈ 1.7 × SWH.

beneath large boulders (Williams and Hall, 2004; Hall et al., 2006) and GIS analysis demonstrating boulder ridge mobility in the absence of tsunami (Cox et al., 2012), there is a growing number of field observations in the wake of large recent storms. Before-and-after image analysis records displacement—at sites well inboard of the high-tide line, and elevations substantially above sea level—of boulders weighing many tens of tonnes (Goto et al., 2009; Fichaut and Suanez, 2011; May et al., 2015; Watkins, 2015; Causon Deguara and Gauci, 2016; Cox et al., 2016; Kennedy et al., 2016a), and also near-sea-level movement of 100 + tonne megagravel (May et al., 2015; Cox et al., 2016; Kennedy et al., 2017). It is increasingly clear that storms can—and do—move large boulders.

But still, direct measurements have been few, and mostly limited to boulders sufficiently large that their pre-storm locations were visible in satellite imagery (May et al., 2015; Kennedy et al., 2016b; Kennedy et al., 2017). These observations open a window on the energies unleashed by storm waves in the coastal zone, but provide little constraint on the way in which those energies dissipate as the ocean waters move inland; nor do they provide insight into the sedimentology and dynamics of CBD in general. To do that requires detailed measurement of clasts at all scales, at a site with precise topographic information, and documentation of CBD configurations both before and after the storm event.

The west of Ireland is that site. From locations along the western coasts (Fig. 3) there are systematic sets of surveyed CBD transects, with associated sedimentologic and photographic data (Zentner, 2009; Cox et al., 2012; Jahn, 2014; Watkins, 2015; Cox et al., 2017), collected in the years before the 2013–2014 storms. We went back out to these sites in the summer of 2014 to see whether the winter storms had wrought any changes. The before-and-after comparisons encompass a spectrum of topographic settings—from the tops of sheer cliffs to low-lying coastal platforms—and also incorporate the full range of boulder sizes, permitting detailed and quantitative sedimentologic analysis. Not only can we show that storm waves move enormous rocks, but by examining the relationships between boulder size and distance from the ocean, we can interrogate how storm wave energy is transmitted inland.

3. Western Ireland's CBD: a classic example

Ireland's high-energy Atlantic coasts (Fig. 3) have several well-developed CBD sites (Williams and Hall, 2004; Scheffers et al., 2009; Cox et al., 2012). The most spectacular examples—with large clast sizes and well developed boulder ridges— occur at Annagh Head in Co. Mayo (Supp. Fig. 1), on the three Aran Islands (Inishmore, Inishmaan, and Inisheer) (examples are shown in Fig. 1, Supp. Figs. 2 and 3), and along the coast between Doolin and Fanore in Co. Clare (e.g. Supp. Fig. 3).

Kinahan et al. (1871) were the first to document these deposits. They reported storm-wave emplacement of boulders up to 53 t mass, but no further work was done until Williams and Hall (2004) described the geomorphology and sedimentology of the Aran Islands boulder ridges. Subsequent studies provided measurements of topographic setting, dimensions, and clast-size distributions of CBD at several locations in Western Ireland (Zentner, 2009; Cox et al., 2012; Jahn, 2014), as well as radiocarbon ages constraining boulder emplacement (Scheffers et al., 2009; Cox et al., 2012). These datasets became the baseline for ongoing annual observations (Zentner and Cox, 2008; Zentner, 2009; Cox et al., 2012; Jahn, 2014; Watkins, 2015), coupled with comparative analysis using historical image sources (Cox, 2013). designed to track changes in the CBD over time.

Each field season revealed limited movement of smaller clasts (up to a few tonnes) and various lines of evidence showed that VLB were clearly shifting on decadal to centennial timescales (Hall et al., 2008; Cox et al., 2012; Cox, 2013). Little of significance, however, was happening in response to the common-or-garden winter storms that happened year-to-year. We were beginning to wonder whether we would ever catch the CBD in the act. But then we got lucky with the 2013–2014 storms.

4. The Winter 2013–2014 “storm factory”

The period November 2013 to March 2014 was exceptionally stormy in northwest Europe, both because of the many closely-spaced storm events and their severity (Matthews et al., 2014; Masselink et al., 2015; Masselink et al., 2016). Wave periods > 20 s were measured off the southwest coast of England, and there were ten storms with peak SWH > 8 m, two of which had peak values greater than 10 m (Masselink et al., 2015). SWH reached 14. 7 m on January 6th, 2014, and an individual wave 23. 4 m high was measured on that day at the M4 buoy off Ireland's NW coast (Gallagher et al., 2016a). Directly west of the Aran Islands, the M6 buoy registered a SWH of 13. 6 m on January 26th, 2014, but broke its moorings in heavy seas shortly thereafter (Marine Institute pers. comm.), and so was out of commission when larger storms directly impacted the Aran Islands the following month. On February 20th, however (during storm Darwin), the Kinsale Energy gas platform off the SW coast registered a 25 m wave against a background SWH of 12 m (Gallagher et al., 2016b). Peak wave periods throughout the winter were unusually long, and associated with record wave heights (Met Éireann, 2014).

Coastal impacts were magnified by storm surge effects. The December 5th “Xavier” storm, for example, coincided with high spring tides, maximising surge and wave heights (Met Éireann, 2014; Wadey et al., 2015). Remarkable coastal geomorphic responses that were reported at the time (e.g. Duell and Brady, 2014; Petley, 2014) attested to the strength of the waves, and suggested that CBD might also have been re-arranged. We therefore mobilised a team to re-visit previously documented CBD sites in western Ireland, with the specific aim of evaluating whether boulder movements had occurred.

5. Methods

In summer 2014 a seven-person field team carried out a comprehensive inventory of boulder transport at 100 survey sites in western Ireland (Fig. 3). Clast movement was measured by comparison with baseline data collected in previous field seasons, so there are two sets of methodologies: the baseline surveys (collected prior to winter 2013–2014), and the post-storm data (collected in summer 2014).

5.1. Baseline transects and photo-documentation

Site surveys (collected between 2008 and 2013) used methods described in Cox et al. (2012). At each location, we recorded the topographic profile and CBD locations (horizontal distance inland and elevation above sea level), as well as heights, widths, and slope angles of boulder ridges. Topographic details were measured using surveying compasses and laser rangefinders. Each survey was anchored by GPS points at the water's edge, the ocean-side base of the ridge, the ridge crest, and the landward end of the deposit. Positional data were time-stamped so they could be corrected for tide height and referenced to local high-water level: all distances and elevations are reported as Above High Water (AHW) (Zentner, 2009; Jahn, 2014). These pre-surveyed transects provide elevation AHW and distance inland for all boulders measured in this study.

Systematic suites of photographs recording boulder arrangements were part of every survey. In each case, a set of photos was taken from the platform near the ridge base, recording the view looking inland, out to sea, and along the ridge in both directions; and a second set was taken from the ridge crest, also in four directions (looking inland, seaward, and up and down the ridge). Additional contextual shots and views were also taken, so that there were 10–20 photographs of the deposits at each surveyed site. The photos were linked to GPS locations. Established sites were visited and re-photographed periodically in subsequent years, resulting in an extensive database of precisely located

Fig. 3. Locations from which data were collected are wide spread on the west coast of Ireland. Base map©maproom.net. Geographic co-ordinates for all locations are given in Supplementary Table 1. The reader can export the latitude and longitude data to Google Earth or Bing Maps to view detailed topography and geomorphology of all sites, or of any specific site.

reference images showing boulder arrangements.

5.2. Post "Storm Factory" field observations

The summer 2014 observations used the pre-2014 photos as baseline data. Using the iPad-based GISKit software, we imported the reference images and linked them to the survey site locations. Field teams navigated to each point using GPS, and then—by comparing the image on the iPad screen with the view in front of them, and adjusting position until objects in the field of view aligned exactly as they did in the photograph—re-occupied the exact stance from which each photograph had been taken (Supplementary Figs. 5–7). By comparing the reference image with the disposition of boulders on-site, we could determine what changes had occurred.

Boulders that had moved within the field of view, or ones that were newly added, were tagged with a number, measured, and recorded. We targeted the largest five or six moved clasts at each site (although where many large rocks had moved we tagged more). The index photo was then re-taken, showing the tagged boulders for subsequent comparison with the original photos (Supplementary Figs. 5–7). Each tagged boulder was measured (X, Y and Z dimensions) and the values entered on a data sheet. The tag number allowed us to associate each measurement on the data sheet with a specific identifiable boulder in the field photograph. In this way we assembled a catalogue of 1153 moved boulders (Supplementary Table 1).

5.3. Estimating boulder size and weight

Boulder masses (Supplementary Table 1) were calculated based on the field measurements of X, Y and Z axis length, and using a density value of 2.61 t/m^3 (measured from hand samples: Jahn, 2014). Clearly—because boulder shapes are not perfectly regular—the volumes thus computed (and hence the masses) are imprecise. Recent studies comparing field approximations with 3D modeling techniques confirm the common-sense expectation that XYZ-based estimates generally overestimate volume (e.g. Spiske et al., 2008; Gienko and Terry, 2014).

But we are not worried about this effect, for two reasons. First, boulders used as examples in the afore-referenced studies are generally

Table 1
Comparing boulder masses based on field measurements (X ∗ Y ∗ Z) with those computed using Structure-from-Motion photogrammetry (SfM). Measured density of 2.66 t/m^3 is used in both cases. Boulder dimensions (X, Y, Z) are given to the nearest 5 cm. An asterisk next to the number indicates that the boulder is in the database of boulders moved during the 2013–2014 storms (Supplementary Table 1). The other six are boulders that appeared on the platform in winter 2015–2016 and were measured for the first time in 2016. Boulder 3 is the isolated platform block in the foreground of Fig. 1.

Boulder	Island	Location	X (m)	Y (m)	Z (m)	Volume X ∗ Y ∗ Z (m^3)	Volume SfM (m^3)	Mass based on XYZ (t)	Mass based on SfM (t)	Difference between masses (%)
1	Inishmaan		2.30	2.20	0.65	3.29	4.01	8.7	9.5	8
2*	Inishmaan		3.30	2.65	0.75	6.56	6.91	17.4	18.4	5
3	Inishmaan		2.75	2.40	1.05	6.93	7.38	18.4	19.6	6
4	Inishmaan	IM 29-IM30	5.50	1.90	0.85	8.88	9.12	23.6	24.3	3
5	Inishmaan		2.35	1.80	0.75	3.17	3.01	8.4	8.0	− 5
6	Inishmaan		2.65	2.25	0.55	3.28	3.17	8.7	8.4	− 3
7*	Inisheer		5.60	2.80	1.80	28.22	28.80	75.1	76.6	2
8*	Inisheer		3.40	2.55	1.10	9.54	11.02	25.4	29.3	13
9*	Inisheer		4.30	2.95	1.35	17.12	15.53	45.6	41.3	− 10
10	Inisheer		4.30	3.05	0.60	7.87	7.71	20.9	20.5	− 2

irregular and/or highly porous, which amplifies the difference between estimated and actual volume. In contrast, the well-lithified, pervasively jointed limestone in our study sites yields boulders with user-friendly orthogonal shapes (Fig. 1, Supplementary Figs. 5–7) such that the X, Y and Z dimensions should yield a good approximation of actual volume; and the measured density (2.61 t/m^3: Jahn, 2014) is about the same as the constituent calcite density, indicating very low porosity. Second, our analysis does not require very accurate mass determinations: in the context of knowing where the largest boulders are moving, the difference between 4 versus 5 t, 18 versus 20 t or 95 versus 105 t is immaterial to our analysis. An error of order 10% in the estimates therefore would not matter.

We tested whether our XYZ-based volume estimates could meet the 10% accuracy criterion by making photogrammetric Structure-from-Motion (SfM) 3D models of a subset of boulders, and comparing the software-computed volumes with those calculated from the field measurements (see e.g. Gienko and Terry, 2014, for a fuller description of this approach). These measurements were collected in 2016, and include some boulders that moved in 2013–2014, but also other boulders, not represented in the 2014 survey (Table 1), that met the criteron for comparative volumetric analysis. To build the SfM models, we needed isolated boulders surrounded by bare platform (see e.g. boulders near cliff edge in Fig. 1A) so that we could capture full 360° imagery unimpeded by obstacles (precise 3D models can't be made if parts of the boulder are occluded by other rocks). We walked around each of these boulders with a GPS-enabled digital camera, taking overlapping images to capture all sides of the boulder, the upper surface, and—to the extent possible—the base (this latter by "duck walking" in a crouch around the rock, imaging as much of the underside as we could). We used Agisoft PhotoScan Pro 1.3.0 to align the georeferenced images and construct precise spatially referenced 3D digital models of the test boulders using standard approaches (e.g. Niederheiser et al., 2016). Comparison of photogrammetric volumes with those estimated from XYZ measurements (Table 1) shows differences ranging from 2 to 10%. Adding 10% error bars to the masses in the data figures would not change any of the trends, so we conclude that the low-tech XYZ tape-measure approach provides sufficiently accurate first-order assessments of boulder volume.

Dimensions of the two largest blocks (Boulders 293 and 297: Fig. 4) had to be measured remotely, because they sit on cliff-base platforms inaccessible without ropes. We flew a Phantom 3 UAV to capture the SfM photogrammetric datasets (e.g. Gienko and Terry, 2014; Zhang et al., 2016), imaging each boulder thoroughly (106 and 175 photos, respectively), with at least 60% overlap between photographs to minimise occlusion and ensure precise modeling.

Creating stand-alone 3D models for objects in a landscape involves interacting with the data, and accuracy therefore is influenced by operator choices as well as data quality. The SfM point cloud must be edited to isolate the object of interest, which involves deleting extraneous points, and in effect carving out the object from its surroundings. Furthermore, boulder undersides are unavoidably occluded where in contact with the bedrock surface. Occlusions manifest as "holes" in the 3D model, requiring extrapolation of surfaces to create a closed solid (Zhang et al., 2016). Exactness of the model therefore depends on how precisely the operator can identify the contact between the boulder and the bedrock when editing the point cloud, and on parameters chosen for the "close holes" procedure in the software. To ensure that we were capturing the uncertainty in the process, we had different operators carry out these procedures several times on each boulder, and report the range of volumes and associated mass estimates for each.

5.4. Measuring boulder displacement

Identifying moved boulders was simple—clasts in new positions were easy to recognise in before-and-after comparisons. But figuring out how far they had moved was trickier, because that involved being able to identify both the original position and the final resting place. In cases where new clasts simply appeared in the archive photograph field of view, it was impossible to determine precisely where they had come from. Similarly, locating boulders that had moved out of the picture was challenging at best. Even rocks that remained within the frame could effectively be disguised if they rotated during transport, presenting a different side to the camera so that we had no chance of recognising them. We measured transport distances only in cases where we could unambiguously identify both the original and final clast locations based on the photographic evidence. We therefore report displacement values for only about a third of the database (374 of the 1153 clasts: Supplementary Table 1).

We used tapes to measure short displacements, and laser rangefinders when transport distances were > 30 m. To determine displacement of the two largest blocks (Boulders 293 and 297: Fig. 4), which are clearly visible in high-altitude orthophotography, we overlaid recent Digital Globe orthoimages (in Bing Maps and on Google Earth) with Ordnance Survey Ireland (OSI) archival aerial imagery,[2] georeferenced and scaled them, and then measured the distance between the starting positions and the post-2014 locations (e.g. Supp. Fig. 8A and B).

6. Results and discussion

We photo-documented dislocation of 1153 boulders across the 100 sites, and recorded dimensions and estimated mass of each (Supplementary Table 1). For 374 of these, we were able to determine

[2] OSI makes historical imagery available online through its GeoHive site: map. geohive. ie/mapviewer. html

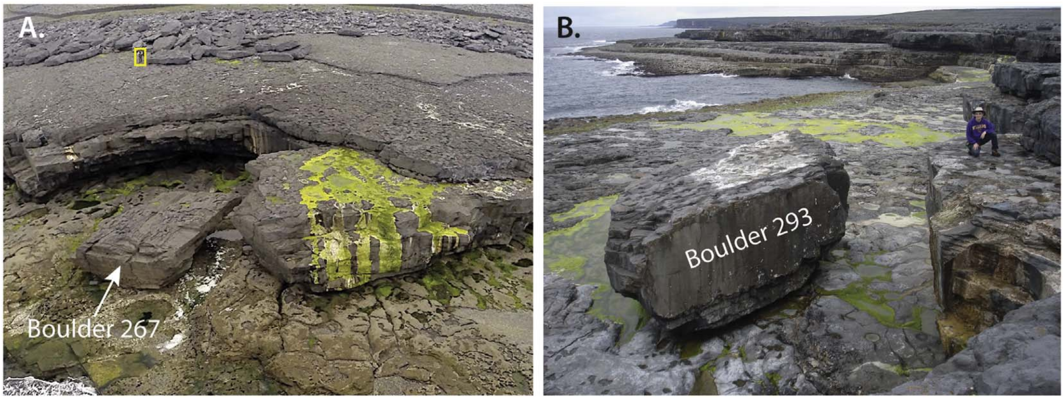

Fig. 4. Feld photographs of the two largest blocks to have moved during winter 2013–2014. Both are on the island of Inishmore. **A**: Boulder 267, on the lower platform, weighs ≈ 475 t. The yellow box outlines two full-size adults on the upper platform. **B**: Boulder 293 weighs ≈ 620 t. The white patch on its upper surface marks the previous location of a 60-ton slab that was dislodged during the recent storms. Supplementary Fig. 4 shows before-and-after location images for both. boulders. See Section 6.2 for details on the mass determinations. The platforms on which these blocks are sitting are close to sea level, but above the high-water mark. The ponds near the boulders are not tide pools, but contain fresh water (made slightly brackish by sea spray), which flows onto the platform via springs emerging along bedding planes in the limestone. The bright green algae in both images are non-marine, salt-tolerant terrestrial species. In **B**, the tide is partially out and the upper intertidal (lowest platform) is visible. In **A**, the tide is almost fully in, and that lowermost platform is inundated.

not just that they had moved, but where they had come from, so in those cases we also report horizontal and vertical travel distances. The amount of activity varied from site to site, ranging from a single moved boulder (at the high-elevation locations 80 and 82, Supplementary Table 1), to forty-two transported clasts (at Location 4). Moved clasts include pre-existing boulders translocated on the coastal platform or redistributed within boulder ridges (e.g. Supplementary Figs. 5, 7, 8), and also boulders newly created from bedrock (e.g. Supplementary Fig. 6).

By combining the data from all 100 sites, we gain a synoptic view of the work done by storm waves over a wide range of elevations and inland distances. No single site includes all settings, but among the sites there are sheer cliffs (e.g. Fig. 1A), broad sloping platforms (e.g. Fig. 1B, Supp. Figs. 1 and 3), and stepped coasts (Supp. Figs. 2 and 4). Thus the dataset provides an integrated view of storm-wave transport capabilities across a wide spectrum of coastal topography. The locations cover many linear km of coastline (Fig. 3). Full data, including geographic co-ordinates, are provided in Supplementary Table 1, and the reader can export the lat-long data to Google Earth, permitting zoomed-in examination of the topographic details of each data-collection site.

6.1. Overview of boulder movements

Masses of moved boulders span several orders of magnitude, from $< 10^{-1}$ to $> 0.5 \times 10^3$ t. Among the moved clasts are eighty-three with masses ≥ 20 t, including eighteen VLB ≥ 50 t. Seven of the boulders are > 100 t. The two largest blocks (Supplementary Table 1, boulder numbers 267 and 293, each weighing several hundred tonnes) are located close to sea level. At greater elevations, the clasts that moved are smaller—but “smaller” is a relative term: boulders up to 20 t mass were transported at 20 m AHW. The highest elevation at which we recorded displacement is 26 m AHW (at 18 m inland, maximum clast size 1.2 t: Location 24 in Supplementary Table 1), and the farthest distance inland is 222 m (at 20 m AHW, maximum clast size 28. 5 t, Location 54).

Some boulders moved very little, others moved 10s of m. The largest horizontal transport distance we measured is 95 m (a 49 t block, which moved from a starting location in the intertidal zone to a final location 2. 3 m AHW and 45 m inland: Boulder 1088 in Supplementary Table 1), and the largest vertical displacement is 4. 5 m (an 18 t boulder that was transported from a ridge base at 17 m AWH to the crest of the ridge, with a starting location 120 m inland, and a final resting place 132 m inland and 21. 5 m AHW: Boulder 745 in Supplementary Table 1).

Among the largest clasts, transport distances range from small nudges to substantial shunts along the coastal platform. In the 50–100 t category, boulders moved as little as 0.5 m (Boulder 1153, a 57 t clast, at 4 m AHW and 15 m inland) and as much as 22 m (Boulder 1095, at 75 t, moved along shore, just above high water and a few m inland). For boulders > 100 t, the minimum transport distance is 2 m (Boulder 1151, a 157 t rock, 3 m AHW and 30 m inland) and the largest translation measured is 23 m (Boulder 261, 210 t at 6 m AHW and 27 m inland).

6.2. The biggest movers

The two largest clasts (Boulders 267 and 293 in Supplementary Table 1; Fig. 4) are located on the island of Inishmore (Fig. 1). Boulder number 267 was tricky to model because its rectilinear shape (Fig. 4A) is somewhat deceptive, and there is a deep undercut beneath the block's southern edge (right-hand side in Fig. 4A). That side is very close to the adjacent cliff, which made it difficult to image with the UAV: we were able to image all parts of the block, but the camera-to-object distance was variable, and with the busy background, that resulted in a noisy point cloud. Repeat iterations of the modeling protocols by different operators returned volumes between 180 and 185 m^3, which (using density of 2.61 t/m^3: Jahn, 2014) correspond to mass in the range 470 to 482 t.

Boulder number 293, being more regular in shape and being farther from the cliff (Fig. 4B), was easier to measure. Repeat models produced consistent volume estimates between 237 and 239 m^3, giving a mass between 619 and 624 t. To be conservative, we rounded the mean mass estimate for each block down to the nearest 5 t. Thus we report 475 t as the representative mass for Boulder number 267, and for boulder number 293 we report 620 t (Supplementary Table 1).

Both the 475 t and the 620 t boulders calved from adjacent rock faces at some unknown point in the past. Both are visible as isolated blocks in OSI 1995 aerial imagery, so we know they have been there for more than twenty years, but they may be much older. The sheer size of these rocks makes verification of their displacement particularly significant, so we show before-and-after image pairs for each in Supplementary Fig. 8. During winter 2013–2014 each was shoved several metres along the supratidal platform: The 475 t block moved about 4 m along shore (just above high water and a few m inland: Supplementary Fig. 8 A,B), and the 620 t block shifted about 3. 5 m seaward (from a starting position ≈ 2. 5 m AHW and 75 m inland: Supplementary Fig. 8C, D).

6.3. Topographic controls on the size of boulders that are transported

To a first approximation, we expect that the greater the elevation and the farther the distance inland, the lower the transmitted wave energy. Boulders close to the ocean should move more readily than hydrodynamically equivalent boulders inland, and the maximum transportable size should decrease the farther you are from the shoreline.

We quantify that by examining relationships between boulder masses and their topographic setting. The biggest boulders repositioned at each study site constrain the maximum energy available at that location. There was a big range of clast sizes at these study sites, and in most cases there were larger, unmoved boulders. We are therefore confident that, for the set of storms in winter 2013–2014, we have accurately captured the relationships between topography and expended wave energy.

6.3.1. Elevation

Unsurprisingly, there is a strong inverse correlation between elevation and maximum boulder mass moved. Blocks weighing hundreds of tonnes are restricted to just a few metres AHW, whereas at the highest elevations the largest clasts were two orders of magnitude smaller (Fig. 5A). A regression analysis using the largest moved boulders at each site yields the exponential relationship:

$$\text{Mass (t)} = 150 * e^{-0.15 * \text{Elevation (m)}} \tag{1}$$

The highest elevation in Fig. 5A is 26 m, but this does not represent the limit for boulder movements: there are CBD at higher elevation in the study areas (up to 50 m AHW: Williams and Hall, 2004; Cox et al., 2012). Although the clasts at elevations > 26 m did not move in this set of storms, they are contiguous with deposits where movement was recorded, so we infer that they are also storm-wave activated, and further infer that future, larger storms will induce activity in those highest CBD.

6.3.2. Distance inland

The relationship between boulder size and distance inland from the high water mark is less simple (Fig. 5B). Maximum boulder mass decreases exponentially, from > 500 t near the shore to something around 20 t at about 120 m inland, given by the relationship:

$$\text{Mass (t)} = 164 * e^{-0.02 * \text{Distance (m)}} \tag{2}$$

The rates of change shown in Fig. 5A and B differ by an order of magnitude: maximum transported boulder mass decreases in proportion to the 0.2 power with increasing elevation, whereas for distance inland the decrease is proportional to the 0.02 power (for elevation in units of metres). This is not too surprising, as it requires more work to hoist mass against gravity than to push it horizontally.

We expected to see the initial strong decrease in maximum size with inland distance, as the inrushing flow loses energy. But beyond 120 m inland, the upper surface of the distribution flattens, and there is no subsequent trend in the data. From 120 to 220 m inland the upper limit on boulder size is consistently ≈ 20–35 t. This flattening of the curve was not predicted.

The topographic context of the data points provides some insight: the suite of locations greater than120 m inland are generally at low elevation relative to their distance from the coast, and these CBD are at the back of broad, very gently sloping coastal platforms (e.g. Fig. 1B). Ocean water this far inland is best modeled as a unidirectional bore (Cox and Machemehl, 1986), analogous to flow generated by greenwater overtopping of decks and seawalls (Shao et al., 2006). As it rushes inland across a shallow coastal platform, the bore is little affected by gravity, and can therefore sustain velocity, or even increase in speed (Cox and Ortega, 2002; Ryu et al., 2007). The inland flattening of the mass-distance curve (Fig. 5B) may therefore be telling us something specific about mass transport in areas with wide planar coastal topography.

6.3.3. Steepness

Neither elevation nor inland distance alone can capture the topographic relationship of a clast to the ocean: a boulder perched 20 m AWH on a cliff top is closer to the ocean than one 20 m AHW at the back of a shore platform. So to incorporate both the vertical and horizontal components of the CBD setting we use the slope ratio (elevation AHW: distance inland) as a measure of the steepness of the boulder setting. This yields the strongest trend in the data: an inverse power-law relationship between steepness and maximum transported mass (Fig. 5C).

$$\text{Mass (t)} = 8.17 * \text{Steepness}^{-0.92} \tag{3}$$

Although we refer to this as "steepness", we emphasise that the slope ratio does not describe an actual gradient: for example, CBD sitting on a level platform 5 m inland from the edge of a vertical 50 m cliff would register a 1-in-5 slope, with a steepness ratio of 5. In fact the cliff is much steeper than that, and the cliff-top platform much flatter. But computing the slope ratio provides a measure of both the superelevation of the storm-water surface above datum and its horizontal travel distance, giving an integrated sense of the overall work being done by the storm waves. The take-home message is that the ability of the wave to transport mass is far greater when the coastal topography is more gentle, and drops of dramatically as steepness increases.

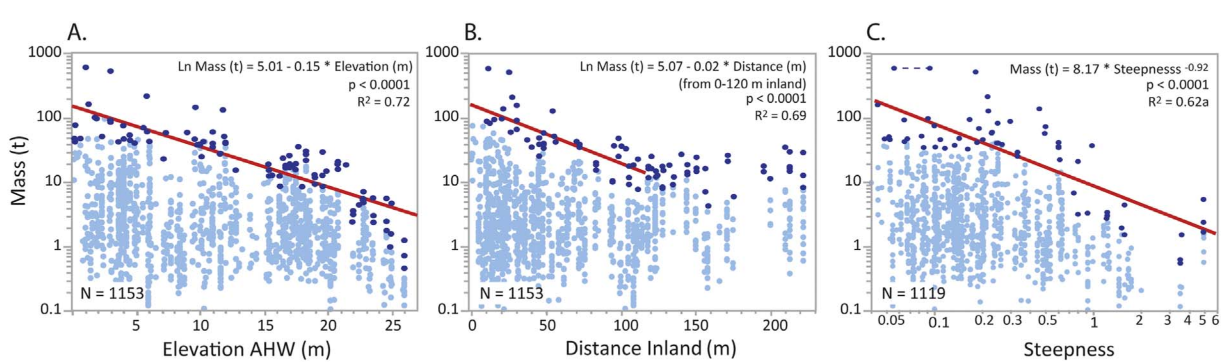

Fig. 5. Masses of transported boulders as a function of topography. Y axis labels in panel **A** apply to all panels. The graphs show all data; the points included in the regression analysis (i.e. the two or three largest masses at each elevation) are highlighted in dark blue. Of the 1153 measured boulders, 41 were excluded from the steepness analysis in panel C: because our topographic measurements are accurate only to about 1 m, steepness estimates are imprecise for locations close to sea level where both elevation and inland distance values approach the error on our measurements. We therefore exclude boulders close to the shoreline, because in those locations our "steepness" estimates are not meaningful. Cutoff values are 10 m inland and 4 m AHW: boulder settings must exceed one or both of those values to be included. Boulder no. 267, one of the two largest clasts moved, barely meets the criteria for inclusion: it is only about 1 m AHW, and its centre of mass is about 11 m inland. The dotted line connecting two points at the upper left corner of the graph shows the range in steepness values for this block based on the limits of topographic accuracy. The different locations of this point do not materially affect the regression line (co-efficients change only in the second decimal place).

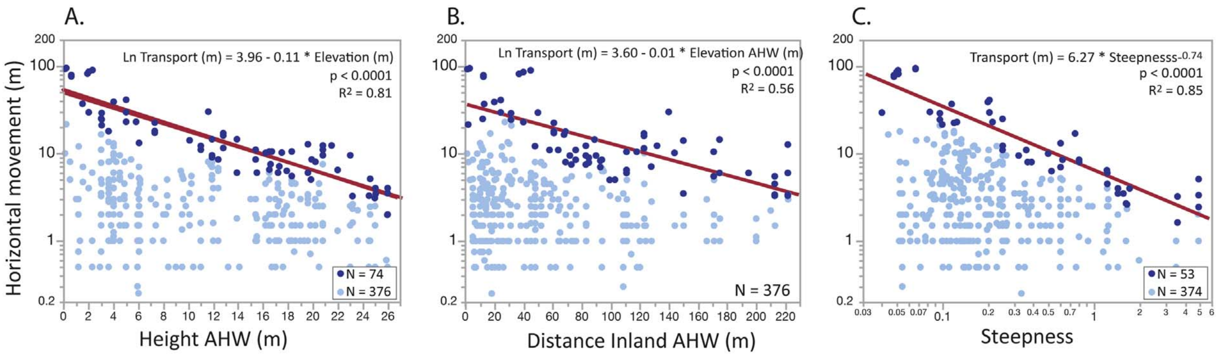

Fig. 6. Horizontal clast transport distance as a function of topographic steepness (elevation AHW/distance inland). Where there is a large distance between the origin and resting place of the clast, the starting topographic setting is used. Total $N = 367$: this is the subset of the dataset for which we were able to measure robust transport distances. The darker points ($N = 24$) are the three highest transport-distance values per X-axis value, and define the upper limits of the data distributions. The regression line through these points provides a relationship between coastal steepness and likely maximum transport distance.

6.4. Topographic controls on how far boulders move

Clasts can move small distances at any elevation and along any kind of slope, but the greater the distance from the fairweather shoreline (vertical or horizontal) or the steeper the coastal profile, the smaller the maximum transport distance (Fig. 6). The effects are strong: all relationships (computed by regression through the dark blue points in Fig. 6, which define the upper bounds on the data) are either exponential (Fig. 6A, B) or power-law (Fig. 6C).

The maximum measured transport distance is 95 m (Boulder 1088: a 41 t clast). This boulder is one of a group (numbers 1088–1094, 35–49 t), all of which were transported > 70 m on a broad, almost horizontal platform close to sea level (sloping 0. 05–0. 07). The farthest-travelled clasts are within a few m of high water: clasts that moved > 50 m are all at elevations below 3 m (Fig. 6A).

But relocation distances at higher elevations are also non-negligible: for example, Boulder 830, a 19 t clast, moved 12 m at 21 m AHW (the location was also 83 m inland). Even at 26 m AHW, we measured transportation distances up to 4 m. There is, however, a dramatic dropoff in maximum transport distance with elevation, defined by the exponential relationship:

$$\text{Transport distance (m)} = 52.5*\text{n}^{-0.11*\text{Elevation (m)}} \tag{4}$$

The relationship between transport length and distance inland (Fig. 6B) is less striking but nonetheless strong. The longest transport paths were closest to the fairweather shoreline (all clasts that travelled > 50 m were located < 45 m inland). Although transport distances decrease further inland, they remain substantial: even at 220 m inland, a 4 t boulder was transported 13 m. The overall decline in maximum transport length with inland distance is, however, exponential. Although the data are noisy ($R^2 = 0.56$), the correlation is highly significant ($p < 0.0001$). The trend is similar to the transport-elevation relationship in Fig. 6A but with an order-of-magnitude smaller exponent:

$$\text{Transport distance (m)} = 36.6*\text{n}^{-0.01*\text{Distance Inland (m)}} \tag{5}$$

In contrast to the boulder mass-inland distance relationship (Fig. 5B), the transport length-inland distance curve does not seem to flatten inland, suggesting (maybe) a progressive decrease in sustained flow strength: although overland bores may be able to budge large boulders at long distances inland, perhaps their ability to maintain the force needed for protracted transport becomes progressively less the farther they are from the shoreline. We recognise, however, that the transport-distance regression line is less steep overall than the mass-distance line (spanning three rather than four orders of magnitude in the Y axis), which, combined with the noise inherent in the data, may be obscuring nuance or detail in the relationships.

There is a power-law relationship between transport distance and steepness (Fig. 6C):

$$\text{Transport distance (m)} = 6.3*\text{Steepness}^{-0.74} \tag{6}$$

which echoes the relationship between boulder mass and steepness (Fig. 5C), and scales similarly. At the steepest sites, the maximum transport was only 4 m. Transport distances > 70 m were achieved only where steepness was < 0.1.

In general, isolated platform blocks racked up the largest transport distances, probably because they were able to skid unimpeded across bedrock. Boulders within ridges tended to move less far, although some that were at the ocean-facing kerbs of boulder ridges moved substantial distances laterally along the front of the ridge. Although some boulders on ridge faces moved downward and oceanward, inland-directed transport was more common: ridge boulders tended to move upward and inland on ridge faces, and some were transferred across ridge crests, ending up on the back of the ridge or even in the scattered boulder field on the landward side (Nagle-McNaughton and Cox, 2016).

7. The dog(s) that didn't bark in the night…

In focusing on the big boulders that moved in the winter of 2013–2014 we should not lose sight of those that stayed exactly where they were. Many big rocks—both isolated platform boulders and clasts within ridges—were unmoved. By remaining in place, these clasts also convey information about CBD dynamics. At most sites, the largest boulders that moved were not the largest available. This means that the biggest rocks that storm waves can transport have not yet been recorded.

The largest coastal boulder we know of (located at 53. 1367°N, 9. 8261°W) is not in Supplementary Table 1 because it stayed absolutely stationary in 2013–2014. With mass estimated at 780 t, this clast sits 25–30 m from the cliff face where it originated. It teeters on a small bedrock step (Fig. 7), demonstrating that is a cliff-detachment block dragged seaward, rather than a fragment stranded by cliff retreat. We do not know at what point in the past this enormous rock was mobilised—nor can we be sure that it was moved by storm waves and not by some long-past tsunami. There are robust sedimentological arguments, however, to suggest that storm waves may have moved it. Size-wise, this block (with Y axis ≈ 11 m) is classified as a medium block (per the criteria of Blair and McPherson, 1999), which is just one size category up from fine blocks, the grade in which the seven largest transported clasts fall. Hydrodynamically, it's not much of a stretch to imagine that storms more energetic than the 2013–2014 events might produce waves capable of moving such a block. We are not asserting that storm waves can do such work, but we are hypothesising that it seems probable. And we will continue to monitor this rock in future years.

Some boulders that should or could have moved, did not budge. Supplementary Fig. 7 shows a block excavated from the subjacent

Fig. 7. This ~780 t cliff-detachment block, at the northwestern end of Inishmore in the Aran Islands, near location 33 (Fig. 3), did not move during the 2013–2014 storms, but was transported to it its current location at some point in the past.

bedrock step and hoisted to lean across the ridge front by storm waves in the past (probably in 1991: Cox et al., 2012). The 2013–2014 storms had no effect on this block, however, despite the fact that, at 78 t, 17 m AHW and 120 m inland, its vital statistics fall well within the moved-boulder zones in the reference parameter spaces (Fig. 5).

The immobility of this clast during storms that moved comparable masses in comparable topographic situations speaks to the stochastic nature of storm-wave transport dynamics. Some CBD express the full capabilities of the storm, and others do not. The angle at which waves approach the shoreline will affect amplification, breaking, and inland bore generation, so different storms can be expected to have varying impact on boulder deposits, depending on coastline orientation (at both the regional and the very local scale). We predict that this boulder (Supplementary Fig. 7) will move in some future storm, and our data (Fig. 5) indicate that—given the right wave approach angle—it could happen with storms no stronger than those of winter 2013–2014.

8. Conclusions and implications

Coastal boulder deposits (CBD) are archives of information about the effects of extreme waves and storm-water incursions along exposed deep-water coasts. Incorporating boulders that weigh in the 10s and even 100 s of tonnes, and located above the high-water mark—some at elevations up to 50 m, some up to a quarter of a km inland—CBD are both spectacular and geomorphologically significant. They represent the inland transfer of extraordinary wave energies. As CBD record the highest energy coastal processes, they are key elements in trying to model and forecast interactions between waves and coasts.

CBD locations, being inhospitable, bear no dwellings and have little infrastructure of any kind, and one might conclude that studying these deposits has little societal relevance. But that would be wrong. Nailing down conditions under which very big boulders are moved is not just about storm impacts on remote coasts: it has direct bearing on understanding storm-coast interactions in the broadest sense. In the first place, measuring these transported boulders reveals the true scale of storm-wave energy. Until very recently, as discussed earlier, it could legitimately be argued that storm waves have not the power to move colossal boulders. We now know that they do, and we measuring CBD allows us to quantify that power.

Second, these data may contribute to hazard modeling for different kinds of coasts under different climate scenarios. Whereas forces this extreme rarely affect the more sheltered coasts where people generally live, that may change. Given that the future may bring increased storminess (Zappa et al., 2013; Brown et al., 2014; Elliott et al., 2014; Slingo et al., 2014) and will surely bring higher sea level, there is an expectation of greater inundation of coastal environments in general (e.g. Vose et al., 2014; Vousdoukas et al., 2016). It is therefore timely to document as well as we can the upper limits of storm wave energy at coasts. Understanding CBD dynamics is essential part of understanding the full spectrum of wave power so that policy makers can plan forward for potential impacts of increased storm energy.

Third, these kinds of data are useful for offshore wave-risk evaluation. Marine locations with abundant wave power, some in the vicinity of this study area (Gallagher et al., 2016b), are targeted for renewable-energy installations. Understanding the forces to which such devices would be subjected is critical (Tiron et al., 2013; Tiron et al., 2015), but direct measurements are difficult, and most high-resolution records are short time series (e.g. Flanagan et al., 2016). The onshore boulder movements preserve a record of forces unleashed at these coasts, and may therefore serve as a proxy for the kind of pounding that near-coast offshore installations might have to endure.

Where CBD occur they provide an eloquent and nuanced record of large-wave events, and their topographic locations are pinning points recording the forces exerted at those elevations and inland distances from the high-water mark. The data presented here underscore that point. The 2013–2014 storms caused boulder dislocation and transport at elevations up to 26 m AHW, and at distances up to 222 m inland (Figs. 5 and 6). Many of the clasts that were transported are very big, including eighteen VLB weighing > 50 t, with six exceeding 100 t. The largest boulder that moved weighs about 620 t. These data show clearly that storm waves have the capacity to do extraordinary work at high elevations and considerable distances from the fairweather shoreline. The boulder mass-topography relationships presented here—and analogous ones that we hope will be generated for other sites and other storm sets in the future—permit extrapolation and estimation of maximum transport capacities. Thus we can better constrain and understand the storm-waves forces to which exposed coasts are regularly subjected.

The boulders moved in western Ireland during the 2013–2014 storms are the largest yet recorded that were unambiguously transported by waves. But we have certainly not yet captured the maximum storm-wave transport capability. At almost every site that we measured there were larger clasts, unmoved by these storms, that had been transported previously by waves. One could argue that large static boulders might be relics of long-past tsunami (Scheffers et al., 2009; Scheffers et al., 2010), but the storms of winter 2013–2014, while many and impressive, were not record-breaking. Stronger individual storms have impacted these coasts in the past (e.g. Shields and Fitzgerald, 1989; Met Éireann, 1991; Cooper et al., 2004) and the 2013–2014 storm sea states were not the greatest on record for the North Atlantic region (Cardone et al., 2011; de León and Soares, 2014; de León et al., 2015). Add to that other records showing wholesale migration of CBD in the last century (Cox et al., 2012), and the conclusion must be that there have been—and will be in the future—storm waves sufficiently energetic to move even larger clasts.

If different storms would move different boulders—and maybe larger ones—do these trends and equations (Figs. 5, 6) have any general applicability? We believe the answer is yes. In areas where both storms and tsunami occur, and where there is debate as to whether CBD are influenced by one or the other, these relationships can serve as a first-order baseline. Areas where storm emplacement has been dismissed because boulder sizes seem too large (e.g. Young et al., 1996; Whelan and Kelletat, 2005; Mastronuzzi et al., 2007; Scicchitano et al., 2007; Barbano et al., 2010; Medina et al., 2011; Mottershead et al., 2014; Prizomwala et al., 2015) can be compared with these data. If clasts fall below the lines of fit in Fig. 5, then storm wave emplacement cannot be dismissed as a potential mechanism.

It is no longer possible, in the face of these data, to conclude that CBD were deposited by tsunami based on boulder mass alone. Hydrodynamic models for boulder transport, which underpinned arguments that storm waves could not move very large boulders (e.g. Young et al., 1996; Nott, 2003b; Noormets et al., 2004), clearly need revision and re-analysis. Similarly, CBD interpreted as tsunamigenic based on hydrodynamic transport equations (e.g. Bryant, 2001; Kelletat et al., 2004; Whelan and Kelletat, 2005; Bryant and Haslett, 2007; Mastronuzzi et al., 2007; Maouche et al., 2009; Barbano et al., 2010; and others) should be re-evaluated. It's entirely possible that tsunami emplaced such deposits; but the interpretation must be based on more diverse sedimentologic criteria, and not on boulder size alone. There is no one-size-fits-all criterion for determining whether a boulder was emplaced by storm waves or tsunami. But if boulder masses plot on or below the reference lines on Fig. 5 A–C, the possibility of storm-wave transport cannot be excluded, and—unless there is strong evidence to the contrary—should probably be the default interpretation.

In the space of just a few years, discussions of boulder transport have flipped from a state where there was no observational evidence for storm wave dislocation of boulders in excess of 50 t (as was pointed out by Scheffers et al., 2009) to the current situation, where new reports of boulders exceeding those criteria are published every year (e.g. May et al., 2015; Kennedy et al., 2016b; Kennedy et al., 2017). The data presented here ratchet the ceiling for storm-wave transport up another notch. We are sure, however, that these new record masses will soon be exceeded, because although the 2013–2014 storms were powerful, from a long-term perspective they were not that special. Stronger storms have hit Ireland in the past and will again: all indicators are that larger boulder movements will be documented in the future.

Documenting boulder creation and transport during these events is one step in a long journey. Showing that storms can move giant rocks is one thing. Understanding the hydrodynamics behind the data is quite another. These data contribute to the growing realisation that CBD are dynamic and that storms are a more powerful sedimentologic force than was hitherto recognised. But we are as yet only scratching the surface, and there is a lot of work still to do.

Supplementary data to this article can be found online at https://doi.org/10.1016/j.earscirev.2017.12.014.

Acknowledgements

This work was possible because of support from NSF awards 0921962 and 1529756, as well as the Williams College Class of 1963 Sustainability Fund. We are also grateful for anonymous reviewer comments on the manuscript. Many Williams College undergraduate students collected field data: baseline measurements were made by Danielle Zentner, Rebecca Gilbert, Brian Kirchner, Nari Miller, Miranda Bona, and David Rapp, and 2014 post-storm movements were recorded by Team Boulder: Kelly Tellez, Kelsey Adamson, Laura Stamp, Jorge Castro, Caroline Atwood and Spencer Irvine.

References

Akrish, G., Rabinovitch, O., Agnon, Y., 2016. Extreme run-up events on a vertical wall due to nonlinear evolution of incident wave groups. J. Fluid Mech. 797, 644–664.
Atan, R., Goggins, J., Harnett, M., Agostinho, P., Nash, S., 2016. Assessment of wave characteristics and resource variability at a 1/4-scale wave energy test site in Galway Bay using waverider and high frequency radar (CODAR) data. Ocean Eng. 117, 272–291.
Autret, R., Dodet, G., Fichaut, B., Suanez, S., David, L., Leckler, F., Ardhuin, F., Ammann, J., Grandjean, P., Allemand, P., 2016. A comprehensive hydro-geomorphic study of cliff-top storm deposits on Banneg Island during winter 2013–2014. Mar. Geol. 382, 37–65.
Barbano, M.S., Pirrotta, C., Gerardi, F., 2010. Large boulders along the south-eastern Ionian coast of Sicily: storm or tsunami deposits? Mar. Geol. 275, 140–154. http://dx.doi.org/10.1016/j.margeo.2010.05.005.
Beisiegel, N., Dias, F., 2017. A Pseudo-spectral Method for Extreme Storm Waves, The 27th International Ocean and Polar Engineering Conference. International Society of Offshore and Polar Engineers: ISOPE-I-17-597.
Blair, T.C., McPherson, J.G., 1999. Grain-size and textural classification of coarse sedimentary particles. J. Sediment. Res. 69, 6–19.
Brennan, J., Clancy, C., Harrington, J., Cox, R., Dias, F., 2017. Analysis of the pressure at a vertical barrier due to extreme wave run-up over variable bathymetry. Theoretical and Applied Mechanics Letters. http://dx.doi.org/10.1016/j.taml.2017.11.001.
Brown, S., Nicholls, R.J., Hanson, S., Brundrit, G., Dearing, J.A., Dickson, M.E., Gallop, S.L., Gao, S., Haigh, I.D., Hinkel, J., Jimenez, J.A., Klein, R.J.T., Kron, W., Lazar, A.N., Neves, C.F., Newton, A., Pattiaratachi, C., Payo, A., Pye, K., Sanchez-Arcilla, A., Siddall, M., Shareef, A., Tompkins, E.L., Vafeidis, A.T., van Maanen, B., Ward, P.J., Woodroffe, C.D., 2014. Shifting perspectives on coastal impacts and adaptation. Nat. Clim. Chang. 4, 752–755. http://dx.doi.org/10.1038/nclimate2344.
Bryant, E.A., 2001. Tsunami—The Underrated Hazard. Cambridge University Press, Melbourne.
Bryant, E., 2014. Tsunami: The Underrated Hazard, Third ed. Springer, United Kingdom.
Bryant, E.A., Haslett, S.K., 2007. Catastrophic wave erosion, Bristol Channel, United Kingdom: impact of tsunami? J. Geol. 115, 253–269.
Bryant, E., Nott, J., 2001. Geological indicators of large tsunami in Australia. Nat. Hazards 24, 231–249.
Burgers, G., Koek, F., Vries, H., Stam, M., 2008. Searching for factors that limit observed extreme maximum wave height distributions in the North Sea. In: Pelinovsky, E., Kharif, C. (Eds.), Extreme Ocean Waves. Springer, Netherlands, pp. 127–138.
Burvingt, O., Masselink, G., Russell, P., Scott, T., 2016. Beach response to consecutive extreme storms using LiDAR along the SW coast of England. J. Coast. Res. 75, 1052–1056.
Buscombe, D., Masselink, G., 2006. Concepts in gravel beach dynamics. Earth Sci. Rev. 79, 33–52.
Carbone, F., Dutykh, D., Dudley, J.M., Dias, F., 2013. Extreme wave runup on a vertical cliff. Geophys. Res. Lett. 40, 3138–3143.
Cardone, V.J., Cox, A.T., Morrone, M.A., Swail, V.R., 2011. Global Distribution and Associated Synoptic Climatology of Very Extreme Sea States (VESS), Proceedings 12th International Workshop on Wave Hindcasting and Forecasting, Hawaii.
Castelle, B., Marieu, V., Bujan, S., Splinter, K.D., Robinet, A., Sénéchal, N., Ferreira, S., 2015. Impact of the winter 2013–2014 series of severe Western Europe storms on a double-barred sandy coast: beach and dune erosion and megacusp embayments. Geomorphology 238, 135–148.
Causon Deguara, J., Gauci, R., 2016. Evidence of extreme wave events from boulder deposits on the south-east coast of Malta (Central Mediterranean). Nat. Hazards 1–26. http://dx.doi.org/10.1007/s11069-016-2525-4.
Cooper, J., Jackson, D., Navas, F., McKenna, J., Malvarez, G., 2004. Identifying storm impacts on an embayed, high-energy coastline: examples from western Ireland. Mar. Geol. 210, 261–280.
Courtney, C., Dominey-Howes, D., Goff, J., Chagué-Goff, C., Switzer, A.D., McFadgen, B., 2012. A synthesis and review of the geological evidence for palaeotsunamis along the coast of southeast Australia: the evidence, issues and potential ways forward. Quat. Sci. Rev. 54, 99–125. http://dx.doi.org/10.1016/j.quascirev.2012.06.018.
Cox, R., 2013. 1930s movie "Man of Aran" as documentary source for studying boulder transport by storm waves. Geol. Soc. Am. Abstr. Programs 45, 52.
Cox, J.C., Machemehl, J., 1986. Overload bore propagation due to an overtopping wave. J. Waterw. Port Coast. Ocean Eng. 112, 161–163.

Cox, D.T., Ortega, J.A., 2002. Laboratory observations of green water overtopping on a fixed deck. Ocean Eng. 29, 1827–1840.
Cox, R., Zentner, D.B., Kirchner, B.J., Cook, M.S., 2012. Boulder ridges on the Aran Islands (Ireland): recent movements caused by storm waves, not tsunami. J. Geol. 120, 249–272. http://dx.doi.org/10.1086/664787.
Cox, R., Watkins, O.G., Tellez, K., Stamp, L.K., Irvine, S.W., Castro, J.A., Atwood, C.E., Adamson, K.P., 2014. Measuring the effects of winter storms (2013–2014) on boulder and megagravel accumulations in western Ireland. Geol. Soc. Am. Abstr. Programs 46, 453.
Cox, R., Jahn, K.L., Watkins, O.G., 2016. Movement of boulders and megagravel by storm waves. Geophys. Res. Abstr. 18 EGU2016–10535. meetingorganizer.copernicus.org/EGU2016/EGU2016-10535.pdf.
Cox, R., Lopes, W.A., Jahn, K.L., 2017. Roundness measurements in coastal boulder deposits. Mar. Geol. http://dx.doi.org/10.1016/j.margeo.2017.03.003.
Dewey, John F., Ryan, Paul D., 2017. Storm, rogue wave, or tsunami origin for megaclast deposits in western Ireland and North Island, New Zealand? PNAS 114 (50), E10639–E10647. http://dx.doi.org/10.1073/pnas.1713233114. (published ahead of print November 27, 2017).
Didenkulova, I., 2011. Shapes of freak waves in the coastal zone of the Baltic Sea (Tallinn Bay). Boreal Environ. Res. 16 (suppl. A), 138–148.
Didenkulova, I., Anderson, C., 2006. Freak waves in 2005. Nat. Hazards Earth Syst. Sci. 6, 1007–1015.
Duell, M., Brady, T., 2014. Obliterated: Cliff Stack Reduced to Sad-looking Pile of Rubble by Raging Seas, Daily Mail, 6 January, United Kingdom.
Earlie, C.S., Young, A.P., Masselink, G., Russell, P.E., 2015. Coastal cliff ground motions and response to extreme storm waves. Geophys. Res. Lett. 42, 847–854.
Met Éireann, 1991. Storm causes death and destruction. Monthly Weather Bulletin 1–5 February issue.
Met Éireann, 2014. Winter 2013/2014. Monthly Weather Bulletin 1–5 December issue.
Elliott, M., Cutts, N.D., Trono, A., 2014. A typology of marine and estuarine hazards and risks as vectors of change: a review for vulnerable coasts and their management. Ocean Coast. Manag. 93, 88–99. http://dx.doi.org/10.1016/j.ocecoaman.2014.03.014.
Emery, K.O., 1955. Grain size of marine beach gravels. J. Geol. 63, 39–49.
Erdmann, W., Kelletat, D., Kuckuck, M., 2017. Boulder Ridges and Washover Features in Galway Bay. Western Ireland, Journal of Coastal Research.
Etienne, S., Paris, R., 2010. Boulder accumulations related to storms on the south coast of the Reykjanes Peninsula (Iceland). Geomorphology 114, 55–70. http://dx.doi.org/10.1016/j.geomorph.2009.02.008.
Felton, E.A., Crook, K.A.W., 2003. Evaluating the impacts of huge waves on rocky shorelines: an essay review of the book 'Tsunami—The Underrated Hazard'. Mar. Geol. 197, 1–12. http://dx.doi.org/10.1016/S0025-3227(03)00086-0.
Fichaut, B., Suanez, S., 2011. Quarrying, transport and deposition of cliff-top storm deposits during extreme events: Banneg Island, Brittany. Mar. Geol. 283, 36–55. http://dx.doi.org/10.1016/j.margeo.2010.11.003.
Flanagan, J.D., Dias, F., Terray, E., Strong, B., Dudley, J., 2016. Extreme Water Waves off the West Coast of Ireland: Analysis of ADCP Measurements, The 26th International Ocean and Polar Engineering Conference. International Society of Offshore and Polar Engineers.
Forget, G., Campin, J.-M., Heimbach, P., Hill, C., Ponte, R., Wunsch, C., 2015. ECCO version 4: an integrated framework for non-linear inverse modeling and global ocean state estimation. Geosci. Model Dev. 8, 3071–3104. http://dx.doi.org/10.5194/gmd-8-3071-2015.
Gallagher, S., Gleeson, E., Tiron, R., McGrath, R., Dias, F., 2016a. Wave climate projections for Ireland for the end of the 21st century including analysis of EC-Earth winds over the North Atlantic Ocean. Int. J. Climatol. 36, 4592–4607.
Gallagher, S., Tiron, R., Whelan, E., Gleeson, E., Dias, F., McGrath, R., 2016b. The nearshore wind and wave energy potential of Ireland: a high resolution assessment of availability and accessibility. Renew. Energy 88, 494–516.
Gienko, G.A., Terry, J.P., 2014. Three-dimensional modeling of coastal boulders using multi-view image measurements. Earth Surf. Process. Landf. 39, 853–864.
Goto, K., Okada, K., Imamura, F., 2009. Characteristics and hydrodynamics of boulders transported by storm waves at Kudaka Island, Japan. Mar. Geol. 262, 14–24. http://dx.doi.org/10.1016/j.margeo.2009.03.001.
Goto, K., Miyagi, K., Kawamata, H., Imamura, F., 2010. Discrimination of boulders deposited by tsunamis and storm waves at Ishigaki Island, Japan. Mar. Geol. 269, 34–45. http://dx.doi.org/10.1016/j.margeo.2009.12.004.
Goto, K., Miyagi, K., Kanawa, T., Takahashi, J., Imanmura, F., 2011. Emplacement and movement of boulders by known storm waves — field evidence from the Okinawa Islands, Japan. Mar. Geol. 283, 66–78. http://dx.doi.org/10.1016/j.margeo.2010.09.007.
Hall, A.M., 2011. Storm wave currents, boulder movement and shore platform development: a case study from East Lothian, Scotland. Mar. Geol. 283, 98–105.
Hall, A.M., Hansom, J.D., Williams, D.M., Jarvis, J., 2006. Distribution, geomorphology and lithofacies of cliff-top storm deposits: examples from the high-energy coasts of Scotland and Ireland. Mar. Geol. 232, 131–155. http://dx.doi.org/10.1016/j.margeo.2006.06.008.
Hall, A.M., Hansom, J.D., Jarvis, J., 2008. Patterns and rates of erosion produced by high energy wave processes on hard rock headlands: the grind of the Navir, Shetland, Scotland. Mar. Geol. 248, 28–46. http://dx.doi.org/10.1016/j.margeo.2007.10.007.
Hall, A.M., Hansom, J.D., Williams, D.M., 2010. Wave-emplaced coarse debris and megaclasts in Ireland and Scotland: boulder transport in a high-energy littoral environment: a discussion. J. Geol. 118, 699–704. http://dx.doi.org/10.1086/656356.
Hansom, J.D., Hall, A.M., 2009. Magnitude and frequency of extra-tropical North Atlantic cyclones: a chronology from cliff-top storm deposits. Quat. Int. 195, 42–52. http://dx.doi.org/10.1016/j.quaint.2007.11.010.
Hansom, J.D., Barltrop, N.D.P., Hall, A.M., 2008. Modelling the processes of cliff-top erosion and deposition under extreme storm waves. Mar. Geol. 253, 36–50. http://dx.doi.org/10.1016/j.margeo.2008.02.015.
Herterich, J.G., Cox, R., Dias, F., 2017. Mechanics of very large boulder creation via hydraulic fracture. Mar. Geol in press.
Hibberd, S., Peregrine, D.H., 1979. Surf and run-up on a beach: a uniform bore. J. Fluid Mech. 95, 323–345. http://dx.doi.org/10.1017/S002211207900149X.
Hibbert-Ware, S., 1822. A Description of the Shetland Islands: Comprising an Account of their Scenery, Antiquities and Superstitions. Constable & Co., Edinburgh.
Hoffmann, G., Reicherter, K., Wiatr, T., Grützner, C., Rausch, T., 2013. Block and boulder accumulations along the coastline between Fins and Sur (Sultanate of Oman): tsunamigenic remains? Nat. Hazards 65, 851–873. http://dx.doi.org/10.1007/s11069-012-0399-7.
Jahn, K.L., 2014. The Sedimentology of Storm-emplaced Coastal Boulder Deposits in the Northeastern Atlantic Region, Geosciences. Williams College, Williamstown, pp. 90.
Kelletat, D., Scheffers, A., Scheffers, S., 2004. Holocene tsunami deposits on the Bahaman Islands of Long Island and Eleuthera. Z. Geomorphol. 48, 519–540.
Kennedy, A.B., Mori, N., Yasuda, T., Shimozono, T., Tomiczek, T., Donahue, A., Shimura, T., Imai, Y., 2016a. Extreme block and boulder transport along a cliffed coastline (Calicoan Island, Philippines) during super typhoon Haiyan. Mar. Geol. http://dx.doi.org/10.1016/j.margeo.2016.11.004.
Kennedy, A.B., Mori, N., Zhang, Y., Yasuda, T., Chen, S.-E., Tajima, Y., Pecor, W., Toride, K., 2016b. Observations and modeling of coastal boulder transport and loading during Super typhoon Haiyan. Coast. Eng. J. 58, 1640004.
Kennedy, A.B., Mori, N., Yasuda, T., Shimozono, T., Tomiczek, T., Donahue, A., Shimura, T., Imai, Y., 2017. Extreme block and boulder transport along a cliffed coastline (Calicoan Island, Philippines) during Super Typhoon Haiyan. Mar. Geol. 383, 65–77.
Kinahan, G.H., Leonard, H., Cruise, R.J., 1871. Explanatory memoir to accompany Sheets 104 and 113 with the adjoining portions of sheets 103 and 122 (Killkieran and Aran sheets) of the Geological Survey of Ireland. Memoirs of the Geological Survey 84.
Kinahan, G., Nolan, J., Leonard, H., Cruise, R., 1878. Explanatory Memoir to Accompany Sheets 93 and 94, With the Adjoining Portions of Sheets 83, 84, and 103, of the Maps of the Geological Survey of Ireland. Memoir of the Geological Survey of Ireland. HM Stationery Office, Dublin available on Google Books. https://books.google.com/books?id=XToiAQAAMAAJ.
de León, S.P., Soares, C.G., 2014. Extreme wave parameters under North Atlantic extra-tropical cyclones. Ocean Model 81, 78–88.
de León, S.P., Bettencourt, J.H., Brennan, J., Dias, F., 2015. Evolution of the Extreme Wave Region in the North Atlantic Using a 23 Year Hindcast, ASME 2015 34th International Conference on Ocean, Offshore and Arctic Engineering. American Society of Mechanical Engineers V003T002A019-V003T002A019.
Lorang, M.S., 2000. Predicting threshold entrainment mass for a boulder beach. J. Coast. Res. 16, 432–445.
Maouche, S., Morhange, C., Meghraoui, M., 2009. Large boulder accumulation on the Algerian coast evidence tsunami events in the Western Mediterranean. Mar. Geol. 262, 96–104. http://dx.doi.org/10.1016/j.margeo.2009.03.013.
Masselink, G., Scott, T., Poate, T., Russell, P., Davidson, M., Conley, D., 2015. The extreme 2013/2014 winter storms: hydrodynamic forcing and coastal response along the southwest coast of England. Earth Surf. Process. Landf. 41, 378–391. https://doi.org/10.1002/esp.3836.
Masselink, G., Castelle, B., Scott, T., Dodet, G., Suanez, S., Jackson, D., Floc'h, F., 2016. Extreme wave activity during 2013/2014 winter and morphological impacts along the Atlantic coast of Europe. Geophys. Res. Lett. 43, 2135–2143.
Mastronuzzi, G., Pignatelli, C., Sanso, P., Selleri, G., 2007. Boulder accumulations produced by the 20th of February, 1743 tsunami along the coast of southeastern Salento (Apulia region, Italy). Mar. Geol. 242, 191–205. http://dx.doi.org/10.1016/j.margeo.2006.10.025.
Matthews, T., Murphy, C., Wilby, R.L., Harrigan, S., 2014. Stormiest winter on record for Ireland and UK. Nat. Clim. Chang. 4, 738–740. http://dx.doi.org/10.1038/nclimate2336.
May, S.M., Engel, M., Brill, D., Cuadra, C., Lagmay, A.M.F., Santiago, J., Suarez, J.K., Reyes, M., Brückner, H., 2015. Block and boulder transport in Eastern Samar (Philippines) during Super typhoon Haiyan. Earth Surf. Dynam. Discuss. 3, 739–771. http://dx.doi.org/10.5194/esurfd-3-739-2015.
Medina, F., Mhammdi, N., Chiguer, A., Akil, M., Jaaidi, E.B., 2011. The Rabat and Larache boulder fields; new examples of high-energy deposits related to storms and tsunami waves in north-western Morocco. Nat. Hazards 59, 725–747. http://dx.doi.org/10.1007/s11069-011-9792-x.
Morton, R.A., Richmond, B.M., Jaffe, B.E., Gelfenbaum, G., 2006. Reconnaissance investigation of Caribbean extreme wave deposits—preliminary observations, interpretations, and research directions. USGS Open-File Report 2006–1293. 46 p.
Morton, R.A., Richmond, B.M., Jaffe, B.E., Gelfenbaum, G., 2008. Coarse-clast ridge complexes of the Caribbean: a preliminary basis for distinguishing tsunami and storm-wave origins. J. Sediment. Res. 78, 624–637. http://dx.doi.org/10.2110/jsr.2008.068.
Mottershead, D., Bray, M., Soar, P., Farres, P.J., 2014. Extreme wave events in the central Mediterranean: Geomorphic evidence of tsunami on the Maltese Islands. Z. Geomorphol. 58, 385–411. http://dx.doi.org/10.1127/0372-8854/2014/0129.
Nagle-McNaughton, T.P., Cox, R., 2016. Inland migration of coastal boulder deposits on Inishmaan, Ireland, measured using structure-from-motion photogrammetry. Geol. Soc. Am. Abstr. Programs 48. http://dx.doi.org/10.1130/abs/2016AM-281197.
Niederheiser, R., Mokroš, M., Lange, J., Petschko, H., Prasicek, G., Elberink, S.O., 2016. Deriving 3D Point Clouds from Terrestrial Photographs-Comparison of Different Sensors and Software. ISPRS-International Archives of the Photogrammetry, Remote Sensing and Spatial Information Sciences, pp. 685–692.
Noormets, R., Crook, K.A.W., Felton, A., 2004. Sedimentology of rocky shorelines: 3.

Hydrodynamics of megalast emplacement and transport on a shore platform, Oahu, Hawaii. Sediment. Geol. 172, 41–65. http://dx.doi.org/10.1016/j.sedgeo.2004.07.006.
Nott, J., 1997. Extremely high-energy wave deposits inside the great barrier reef, Australia: determining the cause—tsunami or tropical cyclone. Mar. Geol. 141, 193–207.
Nott, J., 2003a. Tsunami or storm waves?—determining the origin of a spectacular field of wave emplaced boulders using numerical storm surge and wave models and hydrodynamic transport equations. J. Coast. Res. 19, 348–356.
Nott, J., 2003b. Waves, coastal boulder deposits and the importance of the pre-transport setting. Earth Planet. Sci. Lett. 210, 269–276. http://dx.doi.org/10.1016/S0012-821X(03)00104-3.
Oak, H.L., 1984. The Boulder Beach: a fundamentally distinct sedimentary assemblage. Ann. Assoc. Am. Geogr. 74, 71–82. http://dx.doi.org/10.1111/j.1467-8306.1984.tb01435.x.
O'Brien, L., Dudley, J.M., Dias, F., 2013. Extreme wave events in Ireland: 14 680 BP-2012. Nat. Hazards Earth Syst. Sci. 13, 625–648.
O'Donovan, J., 1839. Letters Containing Information Relative to the Antiquities of the County of Galway, Collected during the Progress of the Ordnance Survey in 1839; Reproduced in 1928 under the Direction of Rev. M. O'Flanagan.
Petley, D., 2014. Remarkable Coastal Change from the Recent UK Storms. American Geophysical Union AGU Blogosphere. http://blogs.agu.org/landslideblog/2014/01/08/uk-storms/.
Prizomwala, S.P., Gandhi, D., Ukey, V.M., Bhatt, N., Rastogi, B.K., 2015. Coastal boulders as evidences of high-energy marine events from Diu Island, west coast of India: storm or palaeotsunami? Nat. Hazards 75, 1187–1203. http://dx.doi.org/10.1007/s11069-014-1371-5.
Richmond, B.M., Watt, S., Buckley, M., Jaffe, B.E., Gelfenbaum, G., Morton, R.A., 2011. Recent storm and tsunami coarse-clast deposit characteristics, southeast Hawai'i. Mar. Geol. 283, 79–89.
Roland, A., Ardhuin, F., 2014. On the developments of spectral wave models: numerics and parameterizations for the coastal ocean. Ocean Dyn. 64, 833–846.
Rueda, A., Camus, P., Méndez, F.J., Tomás, A., Luceño, A., 2016. An extreme value model for maximum wave heights based on weather types. Journal of Geophysical Research (Oceans) 121, 1262–1273.
Ryu, Y., Chang, K.-A., Mercier, R., 2007. Runup and green water velocities due to breaking wave impinging and overtopping. Exp. Fluids 43, 555–567. http://dx.doi.org/10.1007/s00348-007-0332-0.
Santo, H., Taylor, P.H., Gibson, R., 2016. Decadal variability of extreme wave height representing storm severity in the northeast Atlantic and North Sea since the foundation of the Royal Society. Proceedings of the Royal Society A: Mathematical, Physical and Engineering Science 472. http://dx.doi.org/10.1098/rspa.2016.0376.
Scheffers, A., 2002. Paleotsunami evidence from boulder deposits on Aruba, Curaçao, and Bonaire. Science of Tsunami Hazards 20, 26–37.
Scheffers, A., Kelletat, D., 2003. Sedimentologic and geomorphologic tsunami imprints worldwide—a review. Earth Sci. Rev. 63, 83–92. http://dx.doi.org/10.1016/S0012-8252(03)00018-7.
Scheffers, A.M., Kinis, S., 2014. Stable imbrication and delicate/unstable settings in coastal boulder deposits: indicators for tsunami dislocation? Quat. Int. 332, 73–84. http://dx.doi.org/10.1016/j.quaint.2014.03.004.
Scheffers, A., Scheffers, S., Kelletat, D., Browne, T., 2009. Wave-emplaced coarse debris and megaclasts in Ireland and Scotland: boulder transport in a high-energy littoral environment. J. Geol. 117, 553–573. http://dx.doi.org/10.1086/600865.
Scheffers, A., Kelletat, D., Haslett, S.K., Scheffers, S., Browne, T., 2010. Coastal boulder deposits in Galway Bay and the Aran Islands, western Ireland. Z. Geomorphol. 54 (Suppl. 3), 247–279. http://dx.doi.org/10.1127/0372-8854/2010/0054S3-0027.
Scicchitano, G., Monaco, C., Tortorici, L., 2007. Large boulder deposits by tsunami waves along the Ionian coast of south-eastern Sicily (Italy). Mar. Geol. 238, 75–91. http://dx.doi.org/10.1016/j.margeo.2006.12.005.
Shao, S., Ji, C., Graham, D.I., Reeve, D.E., James, P.W., Chadwick, A.J., 2006. Simulation of wave overtopping by an incompressible SPH model. Coast. Eng. 53, 723–735.
Sheremet, A., Staples, T., Ardhuin, F., Suanez, S., Fichaut, B., 2014. Observations of large infragravity wave runup at Banneg Island, France. Geophys. Res. Lett. 41, 976–982. http://dx.doi.org/10.1002/2013GL058880.
Shields, L., Fitzgerald, D., 1989. The 'Night of the Big Wind' in Ireland, 6–7 January 1839. Ir. Geogr. 22, 31–43. http://dx.doi.org/10.1080/00750778909478784.
Siggins, L., 2017. Storm Ophelia: Record 26 m Wave at Kinsale Gas Platform Off South Coast, The Irish Times, October 19th. https://www.irishtimes.com/news/ireland/irish-news/storm-ophelia-record-26m-wave-at-kinsale-gas-platform-off-south-coast-1.3262198.
Slingo, J., Belcher, S., Scaife, A., McCarthy, M., Saulter, A., McBeath, K., Jenkins, A., Huntingford, C., Marsh, T., Hannaford, J., 2014. The Recent Storms and Floods in the UK. 29 p.
Soomere, T., 2010. Rogue waves in shallow water. European Physical Journal Special Topics 185, 81–96. http://dx.doi.org/10.1140/epjst/e2010-01240-1.
Spiske, M., Böröcz, Z., Bahlburg, H., 2008. The role of porosity in discriminating between tsunami and hurricane emplacement of boulders — a case study from the Lesser Antilles, southern Caribbean. Earth Planet. Sci. Lett. 268, 384–396. http://dx.doi.org/10.1016/j.epsl.2008.01.030.
Stevenson, T., 1845. IV—account of experiments upon the force of the waves of the Atlantic and German oceans. Earth and Environmental Science Transactions of The Royal Society of Edinburgh 16, 23–32.
Suanez, S., Fichaut, B., Magne, R., 2009. Cliff-top storm deposits on Banneg Island, Briggany, France: effects of giant waves in the Eastern Atlantic Ocean. Sediment. Geol. 220, 12–28. http://dx.doi.org/10.1016/j.sedgeo.2009.06.004.
Süssmilch, C.A., 1912. Note on some recent marine erosion at Bondi. J. Proc. R. Soc. NSW 46, 155–158.
Switzer, A.D., Burston, J.M., 2010. Competing mechanisms for boulder deposition on the southeast Australian coast. Geomorphology 114, 42–54. http://dx.doi.org/10.1016/j.geomorph.2009.02.009.
Tiron, R., Gallagher, S., Dias, F., 2013. Influence of Coastal Morphology on the Wave Climate and Wave Energy Resource of the West Irish Coast, Proceedings of the 10th European Wave and Tidal Energy Conference Series EWTEC, Aalborg, Denmark.
Tiron, R., Mallon, F., Dias, F., Reynaud, E.G., 2015. The challenging life of wave energy devices at sea: a few points to consider. Renew. Sust. Energ. Rev. 43, 1263–1272.
Tsai, C.-H., Su, M.-Y., Huang, S.-J., 2004. Observations and conditions for occurrence of dangerous coastal waves. Ocean Eng. 31, 745–760. http://dx.doi.org/10.1016/S0029-8018(03)00113-6.
Turton, J., Fenna, P., 2008. Observations of extreme wave conditions in the north-east Atlantic during December 2007. Weather 63, 352–355. http://dx.doi.org/10.1002/wea.321.
Viotti, C., Dias, F., 2014. Extreme waves induced by strong depth transitions: fully nonlinear results. Phys. Fluids 26, 051705. http://dx.doi.org/10.1063/1.4880659.
Viotti, C., Carbone, F., Dias, F., 2014. Conditions for extreme wave runup on a vertical barrier by nonlinear dispersion. J. Fluid Mech. 748, 768–788.
Vose, R.S., Applequist, S., Bourassa, M.A., Pryor, S.C., Barthelmie, R.J., Blanton, B., Bromirski, P.D., Brooks, H.E., DeGaetano, A.T., Dole, R.M., Easterling, D.R., Jensen, R.E., Karl, T.R., Katz, R.W., Klink, K., Kruk, M.C., Kunkel, K.E., MacCracken, M.C., Peterson, T.C., Shein, K., Thomas, B.R., Walsh, J.E., Wang, X.L., Wehner, M.F., Wuebbles, D.J., Young, R.S., 2014. Monitoring and understanding changes in extremes: extratropical storms, winds, and waves. Bull. Am. Meteorol. Soc. 95, 377–386. http://dx.doi.org/10.1175/bams-d-12-00162.1.
Vousdoukas, M.I., Voukouvalas, E., Annunziato, A., Giardino, A., Feyen, L., 2016. Projections of extreme storm surge levels along Europe. Clim. Dyn. 47, 3171–3190.
Wadey, M., Brown, J., Haigh, I., Dolphin, T., Wisse, P., 2015. Assessment and comparison of extreme sea levels and waves during the 2013/14 storm season in two UK coastal regions. Nat. Hazards Earth Syst. Sci. 15, 2209–2225.
Watkins, O.G., 2015. Boulder Movements on the Cliffs of Western Ireland. Geosciences. Williams College, Williamstown, pp. 133.
Whelan, F., Kelletat, D., 2005. Boulder deposits on the southern Spanish Atlantic coast: possible evidence for the 1755 AD Lisbon tsunami? Science of Tsunami Hazards 23, 25–38.
Williams, D.M., Hall, A.M., 2004. Cliff-top megaclast deposits of Ireland, a record of extreme waves in the North Atlantic—storms or tsunamis? Mar. Geol. 206, 101–117. http://dx.doi.org/10.1016/j.margeo.2004.02.002.
Young, R.W., Bryant, E.A., Price, D.M., 1996. Catastrophic wave (tsunami?) transport of boulders in New South Wales, Australia. Z. Geomorphol. 40, 191–207.
Zappa, G., Shaffrey, L.C., Hodges, K.I., Sansom, P.G., Stephenson, D.B., 2013. A multimodel assessment of future projections of North Atlantic and European extratropical cyclones in the CMIP5 climate models. J. Clim. 26, 5846–5862.
Zentner, D., 2009. Geospatial, Hydodynamic, and Field Evidence for the Storm-wave Emplacement of Boulder Ridges on the Aran Islands, Ireland. Geosciences. Williams College, Williamstown, pp. 190.
Zentner, D., Cox, R., 2008. Characteristics and Hydrodynamic Interpretation of Storm-emplaced Cliff-top Boulder Ridges on Inishmore. AGU Fall Meeting Abstracts, Aran Islands, Ireland, pp. 1293.
Zhang, R., Schneider, D., Strauß, B., 2016. Generation and Comparison of TLS and SfM Based 3D Models of Solid Shapes in Hydromechanic Research, Proceedings of the ISPRS-International Archives of the Photogrammetry, Remote Sensing and Spatial Information Sciences, Prague, Czech Republic. pp. 12–19.